CSIRO PUBLISHING

www.publish.csiro.au/journals/pasa *Publications of the Astronomical Society of Australia*, 2003, **20**, 257–262

Long-duration Coherent Radio Emission from the dMe Star Proxima Centauri

O. B. Slee[1], A. J. Willes[2] and R. D. Robinson[3,4,5]

[1] Australia Telescope National Facility, CSIRO, P.O. Box 76, Epping, NSW 2121, Australia
bslee@atnf.csiro.au
[2] School of Physics, University of Sydney, NSW 2006, Australia
willes@physics.usyd.edu.au
[3] Computer Sciences Corporation, 770 Hubble Drive, Lanham Seabrook, MD 20706, USA
[4] Catholic University of America, Washington DC 20064, USA
[5] Department of Physics and Astronomy, Johns Hopkins University,
3400 North Charles Street, Baltimore, MD 21218, USA
robinson@violet.pha.jhu.edu

Received 2003 January 20, accepted 2003 June 03

Abstract: The Australia Telescope and Anglo-Australian Telescope were used in May 2000 to record the radio and optical emissions from the dMe flare star Proxima Centauri. Eight bright optical flares over a two-day interval resulted in no detectable excess short-term radio emission at 1.38 and 2.50 GHz. However, a slowly declining 1.38 GHz emission over the two-day interval was nearly 100% right circular polarised and was restricted to a relatively narrow bandwidth with total intensity (I) and circular polarisation (V) varying significantly over the 104 MHz receiver bandwidth. These are the first observations to show that highly-polarised narrowband flare star emission can persist for several days. This signature is attributed to sources of coherent radio emission in the star's corona. Similarities with various solar radio emissions are discussed; however, it is not possible with the existing observations to distinguish between fundamental plasma emission and electron–cyclotron maser emission as the responsible mechanism.

Keywords: Stars: activity — stars: individual: Proxima Cen — stars: flare — radio continuum: stars — radiation mechanisms

1 Introduction

Considerable effort has been expended over the last 20 years in comparing the various manifestations of stellar and solar activity. It has often been assumed that the two types of activity are qualitatively similar, despite the fact that the energies involved are 3–4 orders of magnitude higher in active stars.

The coherent emissions from the sun such as Type I noise storms, Type III bursts and microwave spike bursts (Dulk 1985), have been so classified on account of their short duration (seconds to milliseconds), high brightness temperature and high degree of circular polarisation. The longest lasting coherent emission from the sun is the Type I noise storm, which can radiate for a day or two, often following a bright solar flare, and consists of many short bursts of varying peak intensity.

The occurrence of coherent emissions from active binaries and flare stars has been recognised principally by the narrow bandwidths, high brightness temperatures, high circular polarisations and comparatively short durations of these events. Because of their low flux densities, it is usually not possible to achieve time resolution of better than a few minutes, although radio flares from the dMe star AD Leo have been detected at 1.4 GHz with completely polarised sub-structure with durations down to 20 milliseconds (Lang et al. 1983; Bastian et al. 1990). Other unambiguous detections of coherent stellar emission at 1.4 GHz have been reported from HR1099 by Jones et al. (1996) and from Proxima Centauri by Lim et al. (1996). The three events seen by Jones et al. lasted from 0.5 to 3 hours, were 100% left-hand circularly polarised (LCP) and were not detected at 2.38 GHz; no pronounced burst-like structure was evident with their 12-minute time resolution. The burst seen by Lim et al. lasted 8 minutes, had 100% LCP and was not detected at 2.28 GHz. Lang & Willson (1986; 1988) found that YZ CMi emitted a continuously variable, completely polarised signal with a fractional bandwidth as low as 0.02, which they attributed to electron–cyclotron masering. The authors of the above papers have variously ascribed their results to either plasma radiation or to cyclotron maser emission. If the latter is operating, one would expect the maser to saturate on millisecond time scales, thus producing bursty emission. Such morphologies have been occasionally detected in solar emission, but the closest analogy in flare star emission is that reported above from AD Leo. Fine structure on the millisecond scale would have been missed by synthesis observations such as those of Jones et al. (1996), since their basic integration times are about 10 seconds; the polarised flux density would have been about 50 times the rms noise even for an integration time of 100 milliseconds, and so millisecond structure would have been detectable had a short enough integration time been available.

Our experiment in May 2000 was primarily designed to investigate the correlation between optical and radio flares from Proxima Cen as observed by the 3.9 m

 10.1071/AS03011 1323-3580/03/03257

Anglo-Australian Telescope (AAT) and Australia Telescope Compact array (ATCA) respectively. As a result of the analysis of the ATCA data, a consistent level of highly polarised 'quiescent' emission was found, persisting over the two days of observation. Section 2 describes the radio and optical observations and data reduction. Section 3 gives the results of the experiment, while Section 4 discusses the correlation between optical and radio flares. Possible mechanisms that may account for such prolonged coherent emission are discussed in Section 5.

2 Observations

2.1 Radio Observations

The ATCA observed Proxima Cen at 1.384 and 2.496 GHz on May 14 and 15, 2000 for 14 hours centred on transit each day. The configuration of the ATCA was such that a bi-modal distribution of spatial frequencies (uv coverage) resulted from the ten baselines from five close-spaced antennas and the five baselines involving the sixth antenna at a distance of 2.5 km from the compact group. We found that the more reliable measurements resulted from using the five long baselines, due mainly to the confusing effects of strong nearby field sources and the presence of some interference on the short baselines, especially at 2.496 GHz. Data runs of 30 minutes were obtained at 1.384 and 2.496 GHz simultaneously, with a sampling time of 10 seconds and were interlaced with 2-minute observations of a nearby phase calibrator.

The uv data from the five long baselines were first used to construct cleaned maps utilising the whole night's data. In order to reduce the deleterious affects of nearby field sources, we found it useful to model the field from its clean components (masking the small area around Proxima Cen) and then subtracted the model to obtain uv data that was substantially free of the field sources. From the maps we were able to obtain an accurate position for Proxima Cen and its offset from the field centre, which was used in the MIRIAD task UVFIT to measure flux densities obtained with integration times of 30 and 4 minutes.

2.2 Optical Observations and Data Reduction

The optical data were obtained on 2000 May 14 (UT 08:25–17:51) and 2000 May 15 (UT 08:47–18:38) using the AAT. The observations consisted of time sequences of spectra taken with a Tektronix (1024 pixel) CCD detector mounted on the 25 cm camera of the RGO spectrograph. The spectra covered a wavelength range of 3390–4970 Å with a 1.547 Å/pixel resolution.

The time sequences were obtained using the rapid readout observing mode. In this mode it is possible to obtain sequences of CCD images, stacking each image into a 3D array. To decrease the readout time between exposures, the data were binned on the detector so that all starlight was contained in the central three rows. A window was then defined so that only nine binned rows were retained upon readout. This window was centred on the star and was wide enough so that the edges gave reasonable sky samples. With these provisions it was possible to reduce the overhead between exposures to 1.5 seconds. We therefore adopted a 4.5 second exposure time and obtained a 6 second time step. To avoid overly large data cubes it was decided to limit the individual time sequences to 30 minutes in duration. It took approximately 30 seconds of overhead to complete one time sequence and start the next. Bias and flat field frames were obtained with the same observing setup and the star Feige 110 was observed as the spectrophotometric standard. The data were reduced at the Anglo-Australian Observatory using the FIGARO data reduction package. Each image in the data cubes was bias subtracted, flat fielded and cleaned of cosmic ray events. Star and sky spectra were then extracted and, after suitable scaling, the sky was subtracted. Wavelengths were determined using Cu–Ar calibration lamp exposures taken during the night and the wavelength scale was linearised. The reduced spectra were then placed into 2D arrays showing fluxes as a function of wavelength and time.

On both nights the seeing ranged between 1.5 and 4.0 arcsec and there were scattered clouds present, especially on May 14. To preserve the spectral resolution the slit width was set to 2 arcsec, so the dataset was not photometric. However, we were careful during the observations to ensure that the slit was orientated as closely as possible to the paralactic angle, so that the atmospheric dispersion was parallel to the slit. Thus we were able to assume that the effects of seeing and extinction are effectively independent of wavelength. Flares, on the other hand, are known to be substantially bluer than the star. We therefore searched for flares by using the flux in the 4600–4820 Å region as a reference and looked for variations in the 3500–4000 Å region. This region contains the strong Ca II resonance lines as well as most of the high order Balmer lines and the Balmer continuum, many of which show pronounced increases during flares.

3 Results

3.1 The Radio Results

Table 1 shows the dates and durations of the observations and the mean daily flux densities with their 1σ errors. The lack of a detection at 2.496 GHz (the upper limits are 3σ) implies that either the emission has a very steep spectral index or has a relatively narrow bandwidth near 1.384 GHz. If the former is true, the spectral index between 1.384 and 2.496 GHz was $\alpha < -4.6$ on May 14 and $\alpha < -2.8$ on May 15, where flux density is proportional to ν^{α}. Such a spectral index is far higher than would be expected from gyrosynchrotron emission in the optically thin regime. The high right-handed circular polarisation (RHC) at 1.384 GHz on both nights lends further support for narrowband coherent emission. There is already evidence of high circular polarisation in a very short 1.384 GHz flare from Proxima Cen (Lim et al. 1996), but the present observations are the first to show that such coherent emission can last for at least two days.

https://doi.org/10.1071/AS03011 Published online by Cambridge University Press

Table 1. Average Flux Densities for Proxima Centauri

Date	UT Interval (h:m)	Mean Flux Density (mJy)			Polarisation 1.384 GHz (%)
		1.384 GHz (I)	1.384 GHz (V)	2.496 GHz (I)	
14/5/00	06:14–20:20	2.74 ± 0.08	2.62 ± 0.07	$\leq 0.18^a$	96 ± 5
15/5/00	09:06–20:16	1.55 ± 0.09	1.29 ± 0.07	$\leq 0.29^a$	83 ± 9

[a] Upper limits at 2.496 GHz are $3 \times$ rms.

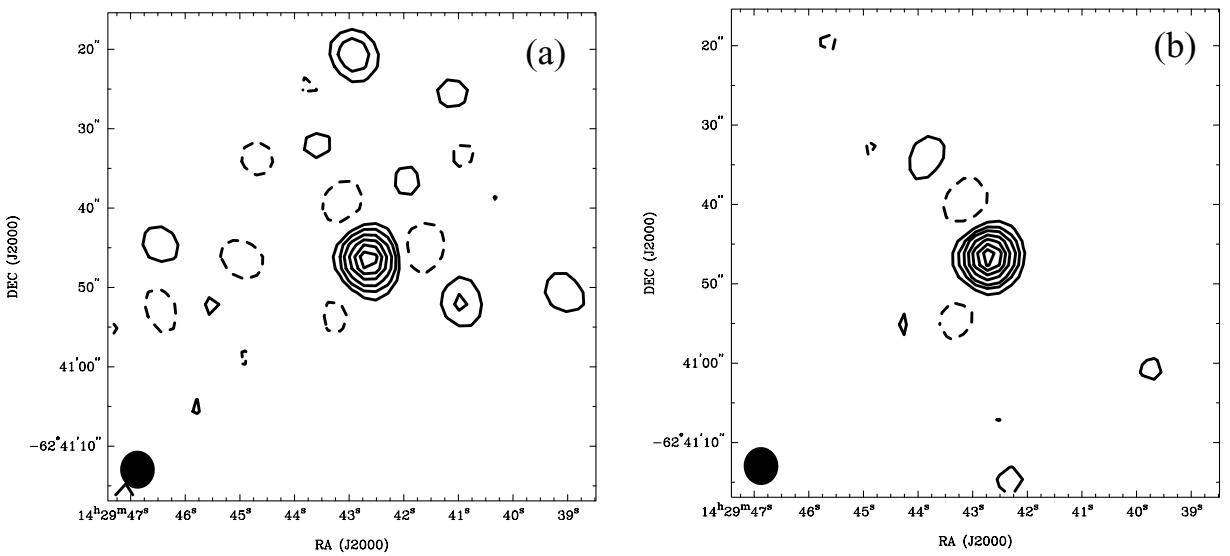

Figure 1 Contours of radio brightness at 1.384 GHz. The lowest contour corresponds to 0.23 mJy beam^{-1}, the brightest to 2.05 mJy beam^{-1}. Panel (a) shows total intensity (I) and panel (b) shows the circularly polarised brightness (V). The sense of polarisation is right handed. The restoring beam in the bottom left corner is $4.8'' \times 4.4''$ to half-brightness in PA = 2.0 degrees.

The total intensity (I) and circular polarisation maps (V) are shown for the data of May 14 in Figure 1. It is clear that the I and V brightness distributions for Proxima Cen are very similar and consistent with those of a point source, the only significant difference arising from the presence of two additional weak sources on the I map.

Figure 2 is a plot of the I and V flux density at 1.384 GHz from 30-minute integrations on the two nights of observation. The emission intensity clearly decreases slowly over the two-day interval with the regression line consistent with the measured daily averages in Table 1. The degree of correlation between I and V is probably as high as one could expect given the large 1σ error bars and a probable calibration error in V at some hour angles. There is no compelling evidence for short-term variability in I within the 14-hour run of data. A break-down of the data into 4-minute integrations (not shown) does not indicate stronger variability on the shorter time scale, although it could be present but masked by the three-fold increase in rms noise.

There is evidence for variation in I, V and V/I over the 104 MHz passband of the receiver. Figure 3 shows the intensities measured in 12 independent IF channels each 4 MHz wide and 8 MHz apart, with one channel missing at 1408 MHz. This plot utilises the data from the whole 14 hour session on May 14. It shows that the

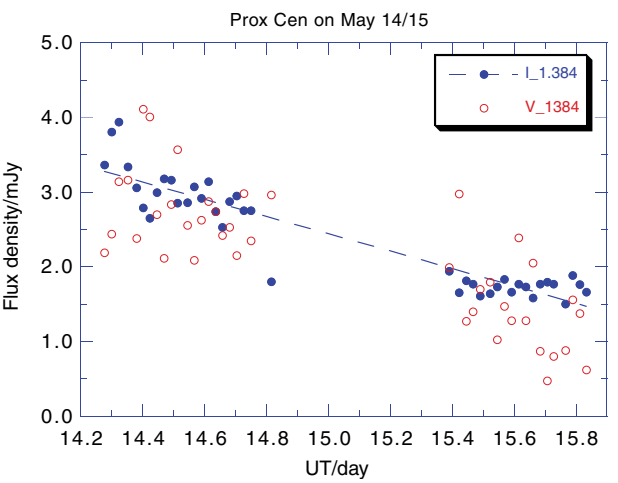

Figure 2 Half-hourly integrations of the high-resolution uv data over the two-day observation. The linear regression line for I is shown.

total intensity (I) drops by a factor of two over the pass band while the polarised intensity (V) drops by a factor of four; therefore the polarised fraction (V/I) is reduced from ∼1 at 1328 MHz to ∼0.5 at 1432 MHz. A similar analysis of the uv data from the calibrator (two-minute

https://doi.org/10.1071/AS03011 Published online by Cambridge University Press

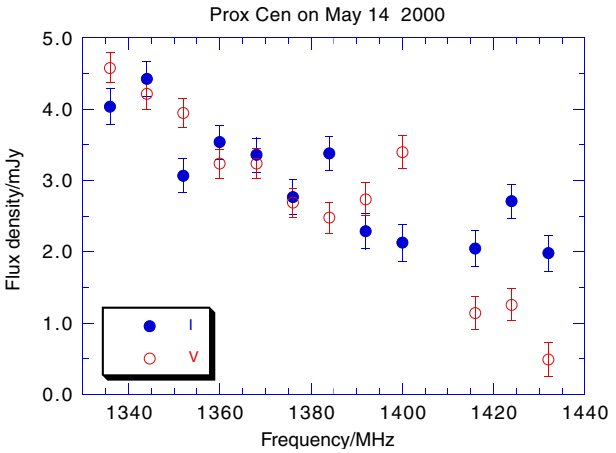

Figure 3 Total intensity (I) and polarised intensity (V) in 12 bands occupying the 104 MHz bandwidth of the receiver. One band at 1408 MHz is missing. The bands are 4 MHz wide and their centres are 8 MHz apart. The *uv* data encompasses the 14 hours of the observation.

integrations interposed between those of Proxima Cen) yielded a mean channel intensity with a standard deviation of 0.07%, thus showing that there is no significant instrumental error across the 104 MHz bandwidth. There is here additional evidence for the narrowband nature of the polarised emission, with the presence of a 2/1 variation in flux density across our passband implying that we are beginning to resolve frequency structure in the emission with a fractional bandwidth not much greater than 0.07. An unsuccessful attempt was made to identify finer frequency structure that could be present in individual 30-minute integrations. The large variability in channel intensity that was measured is almost certainly due to calibration error introduced by the method of calibration in MIRIAD. This was verified by finding much greater variability than expected (from the increase in system noise) across the passband in short sections of calibrator data.

3.2 The Optical–Radio Correlation

During the two nights we obtained a total of 1230 minutes of data, of which 415 minutes were too heavily affected by clouds to reliably detect flares. In the remaining 815 minutes we confidently detected 8 flare events. The properties of these flares are presented in Table 2. In all cases they were simple bursts, with sharp impulsive phases lasting less than 15 seconds, total durations of less than 4 minutes and peak enhancements ranging from 0.5 to nearly 2 magnitudes. Smaller flares are probably present, but the short durations and poor observing conditions did not allow us to make reliable identifications.

None of the 4-minute radio integrations over these flaring intervals showed a significant increase in flux density. The 3σ detection limit at both 1.384 and 2.496 GHz was $\approx$3.0 mJy in both I and V flux densities. The literature on the subject of optical–radio flare correlation is replete with contradictions. Our own results (in preparation) involving AAT and 4-frequency ATCA observations of the dMe star YZ CMi, yielded excellent correlations with 4.8 GHz and 8.64 GHz flares, but no definite correlations at 1.384 and 2.964 GHz. Therefore, our evidence is that Proxima Cen and YZ CMi, stars of the same spectral type, show similar behaviour with respect to dependence of correlation on frequency. One tentative interpretation for the lack of an optical–radio flare correlation at 1.4 GHz is that the electrons that are accelerated to sub-relativistic energies in the low corona at the time of a flare do not penetrate into the higher corona, from which the lower radio frequencies can escape.

Table 2. Optical flare parameters

Date	Start	Peak Enhancement (mag)	Total Duration (sec)
2000 May 14	11:55:40	1.8	250
2000 May 14	16:56:00	1.4	180
2000 May 15	11:48:05	1.1	30
2000 May 15	13:14:50	0.5	120
2000 May 15	14:26:10	1.0	300
2000 May 15	16:00:40	1.1	150
2000 May 15	16:30:20	0.8	65
2000 May 15	19:13:30	0.9	90

4 Power and Brightness Temperature

The parallax measurement from Hipparcos gives a distance to Proxima Cen of 1.295 pc. The 1.384 GHz power emitted at the start of May 14 was 6.0×10^5 W Hz^{-1} into 4π sr. The stellar radius is 0.15 $R_\odot$ (Pettersen 1980) leading to a brightness temperature $T_b = 2.4 \times 10^9$ K for a source occupying the whole stellar disk. By the end of the second day (see Figure 2), both power and brightness temperature had dropped by a factor of 2.4. Since the high degree of polarisation and the relatively small bandwidth suggest that the source is coherent, it is likely that the projected source area is much lower than that of the stellar disk with a corresponding increase in brightness temperature.

5 Discussion

Lang & Willson (1986; 1988) reported observations of coherent narrowband radiation from YZ CMi, which persisted throughout the 4-hour observation time. These observations show many similar properties to the long-duration emission from Proxima Cen reported here; namely, (i) Long durations and intensity variations on minute time scales. The intensity variations are more pronounced for the emissions from YZ CMi than from Proxima Cen. (ii) High degrees of circular polarisation. The YZ CMi emissions are also nearly 100% LCP. However, without knowledge of the predominant magnetic field polarity of the active region producing the radiation, the polarisation mode (*x*-mode or *o*-mode) cannot be ascertained from the observed handedness. (iii) Narrow bandwidths. Lang & Willson (1988)

https://doi.org/10.1071/AS03011 Published online by Cambridge University Press

divided the 50 MHz bandwidth of the VLA into 15 contiguous 3.125 MHz channels, and found several 10-minute time intervals with bandwidths $\Delta\nu \approx 30$ MHz and $\Delta\nu/\nu \approx 0.02$. They hypothesised that the broader-band spectra detected in other time intervals, with unresolved bandwidths $\Delta\nu > 50$ MHz, consist of a superposition of multiple narrowband bursts with different central frequencies. In contrast, the long-duration coherent radiation from Proxima Cen exceeds the 104 MHz bandwidth of the ATCA, with $\Delta\nu/\nu > 0.07$. One possible explanation for the unresolved bandwidth for Proxima Cen is that the Proxima Cen source region consists of a larger number of individual emission sources over a range of central frequencies than YZ CMi. Consequently, time intervals of resolved bandwidth (with $\Delta\nu < 100$ MHz) are less likely to be observed. This scenario is also consistent with the weaker intensity variation over minute time scales for Proxima Cen, in comparison with YZ CMi.

There are two known emission mechanisms which can account for these properties of long-duration emissions from Proxima Cen and YZ CMi: electron–cyclotron maser emission (ECME) and plasma emission. Both of these mechanisms are responsible for a variety of solar radio emissions. The first of these, ECME, naturally explains the high polarisation, narrow bandwidth, and constant emission frequency of the long-duration narrow band events from Proxima Cen and YZ CMi (Lang & Willson 1986; 1988). One necessary condition for an electron–cyclotron maser to operate is that the source region plasma has a relatively low plasma density and/or a relatively high magnetic field strength, such that the ratio of the electron plasma frequency to the electron–cyclotron frequency is small, with $\omega_p/\Omega_e \lesssim 1$. For $\omega_p/\Omega_e \ll 1$, the highest maser growth rate is in the x-mode at the fundamental ($\omega \approx \Omega_e$). However, it is highly likely that fundamental maser emission is reabsorbed as it propagates into harmonic absorption bands in regions with lower magnetic field strengths (Melrose & Dulk 1982). Reabsorption is significantly weaker for maser emission produced at higher cyclotron harmonics. Consequently, the strongest maser emission likely to reach an observer is x-mode emission at the second harmonic (Melrose & Dulk 1982), although higher harmonics are also possible, depending on the system parameters. Second-harmonic maser emission at 1.4 GHz corresponds to a source region field strength of 250 G, and the condition $\omega_p/\Omega_e \lesssim 1$ then requires source region plasma densities $n_e \lesssim 6 \times 10^9$ cm^{-3} (Lang & Willson 1986).

There are no solar ECME events analogous to long-duration flare star emissions which persist on time scales of days. ECME is the favoured mechanism for solar microwave spike bursts, which are produced in the frequency range 0.3–3 GHz with high degrees of circular polarisation. Spike bursts occur on time scales of seconds to minutes, and comprise many individual spikes, which typically have time scales of tens of milliseconds. Fine temporal structure on millisecond time scales has been detected in radio flares from other flare stars (Lang et al. 1983; Bastian et al. 1990). However, the long-duration narrowband emissions from Proxima Cen are unlikely to be directly analogous to solar decimetric spike bursts. Solar decimetric spike bursts are strongly correlated with hard X-ray bursts (Benz & Kane 1986), which are produced in association with energetic electrons accelerated in solar flares. In contrast, the long-duration Proxima Cen emissions do not appear to be correlated with optical flares.

The second mechanism is plasma emission, which operates in the parameter regime with $\omega_p/\Omega_e \gtrsim 1$. In a two-stage process, a beam instability generates electrostatic waves, which are subsequently converted to free space modes via nonlinear wave–wave processes. Examples of plasma emission in the solar context include type II and type III radio bursts, where electron-beam generated Langmuir waves are converted to fundamental ($\omega \approx \omega_p$) and second harmonic radiation via three-wave interactions involving low-frequency ion sound waves (Melrose 1985), and multiple-frequency-band solar decimetric spike bursts associated with electron Bernstein waves (Willes & Robinson 1996). Harmonic plasma emission tends to have moderate degrees of circular polarisation, favouring both x-mode and o-mode emission in different parameter regimes (Willes & Melrose 1997; Willes 1999). In contrast, fundamental plasma emission is 100% polarised o-mode emission, although depolarisation effects are often significant in the solar context. Thus, if long-duration flare star emissions at 1.4 GHz are produced by plasma emission, it is most probably fundamental plasma emission, corresponding to a coronal source region plasma density $n_e \approx 2.5 \times 10^{10}$ cm^{-3}.

The class of solar radio emission most analogous to long-duration flare star emissions are type I storms, which are generated at metric frequencies (150–350 MHz). Type I storms possess high degrees of polarisation and consist of many individual type I bursts superposed on lower-level continuum emission. They have long durations ranging from hours to several days, and individual type I bursts have narrow bandwidths ($\Delta\nu/\nu \lesssim 0.03$) and time scales of seconds. One proposed explanation for the continuum emission, which has a broader bandwidth than individual bursts, is that it consists of a superposition of large numbers of lower-intensity type I bursts (Kai et al. 1985). One proposed explanation for the partial association of type I storms with flares is that type I storms are produced in association with emerging magnetic flux in active regions, which occurs both during flares and in quieter periods (Spicer et al. 1981). This is indicative of continuous electron acceleration, rather than an association with the more transient energetic electrons produced in flares. There is no one widely supported theory for solar type I emission, although the observed o-mode polarisation is indicative of fundamental plasma emission, and the constant emission frequency is consistent with a source region in which energetic electrons are trapped in constant density regions within closed magnetic structures above active regions (Melrose 1980). Constant-frequency emissions from Proxima Cen are less likely to be analogous to other classes of solar radio emission (type II, III and

https://doi.org/10.1071/AS03011 Published online by Cambridge University Press

IVM bursts) which typically exhibit decreasing emission frequencies with time as the radiation source moves out towards lower coronal plasma densities (Lang & Willson 1988), and which tend to have low degrees of circular polarisation.

Over the two days of observation, the coherent emissions from Proxima Cen gradually decrease in intensity. This decay timescale may be the characteristic timescale of the 'storm' emission on an active region on Proxima Cen, or alternatively may be due to the active region rotating out of view, where the two-day observing time constitutes a small fraction of Proxima Cen's ∼41 day rotation period. Prior ATCA observations of Proxima Cen (Lim et al. 1996) suggest that Proxima Cen is a prolific generator of radio emission at 1.384 GHz. Observation of both short-duration and long-duration narrowband emissions from Proxima Cen at different observation times (ten years apart) can be interpreted as either being due to temporal variation of the level and topology of stellar magnetic activity between the two observing periods (in analogy to the solar cycle) or being due to a strong spatial dependence of the active region morphology and flaring behaviour. Longer continuous observing times of Proxima Cen are required to distinguish between these possibilities.

The flux density integrated over one 14-hour observing period decreases with increasing frequency across the 104 MHz ATCA bandwidth. This suggests that the peak emission frequency lies below 1330 MHz. It also appears that the degree of circular polarisation is significantly reduced at the lowest flux densities in the highest frequency bands. It is difficult to interpret this without observations over the full bandwidth of emission. However, by analogy with solar radio emissions, it is likely that depolarisation and mode coupling effects can lower the observed degree of polarisation. These observations are also consistent with the conjecture that quiescent radio emission from dwarf M stars consists of a superposition of large numbers of low-level coherent bursts (Lang & Willson 1988). In this scenario, the degree of polarisation is expected to decrease with flux density.

6 Conclusions

We have detected the presence of a two-day 'quiescent' emission at 1.38 GHz that is nearly 100% circularly polarised (RHC). Our basic integration time of 10 seconds prevents us from searching for burst-like structure on millisecond time scales, which is known to be present in solar spike bursts and, for short intervals, in one or two other active stars.

Our evidence for a coherent mechanism is derived from the radiation being clear at 1.38 GHz, but not detected at 2.50 GHz, combined with a 2/1 variation in total intensity and polarised fraction over the receiver bandwidth of 104 MHz centred on 1.38 GHz in one of our 14-hour integrations. This suggests that there is frequency structure present of the order of 7% of the observing frequency.

The fact that there were no increases in the polarised emission at or following any of the eight optical flares, indicates that there may be a different coherent mechanism operating in Prox Cen than those responsible for Type I noise storms and microwave spike bursts in the sun, which often (but not always) follow solar flares. However, one must keep in mind that a stellar flare may excite an additional coherent source but with emission in a narrow frequency band that was not under observation. Based on our present knowledge of coherent radiation mechanisms, the emission is either fundamental plasma emission or electron–cyclotron maser emission.

Further progress in the interpretation of stellar coherent emission depends upon our ability to modify the hardware of synthesis telescopes to record much shorter integrations of say 100 milliseconds, which could be achieved at acceptable signal-to-noise on the occasional strong coherent bursts from an active star such as HR1099. The better time resolution, coupled with an order of magnitude increase in frequency resolution, should enable us to distinguish between plasma emission and electron–cyclotron masering.

Acknowledgements

The Australia Telescope Compact Array is part of the Australia Telescope, which is funded by the Commonwealth of Australia for operation as a National Facility managed by CSIRO. We thank Dr G. S. Tsarevsky for his help with the radio observations. AJW acknowledges support from the Australian Research Council through an Australian Postdoctoral Research Fellowship.

References

Bastian, T. S., Bookbinder, J. A., Dulk, G. A., & Davis, M. 1990, ApJ, 353, 265
Benz, A. O., & Kane, S. R. 1986, Sol. Phys., 104, 179
Dulk, G. A. 1985, Ann. Rev. Astron. Astrophys., 23, 169
Jones, K. L., Brown, A., Stewart, R. T., & Slee, O. B. 1996, MNRAS, 283, 1331
Kai, K, Melrose, D. B., & Suzuki, S. 1985, in Solar Radiophysics, eds D. J. McLean & N. R. Labrum, (Cambridge: Cambridge University Press), 415
Lang, K. R., Bookbinder, J., Golub, L., & Davis, M. 1983, ApJ, 272, L15
Lang, K. R., & Willson, R. F. 1986, ApJ, 302, L17
Lang, K. R., & Willson, R. F. 1988, ApJ, 326, 300
Lim, J., White, S. M., & Slee, O. B. 1996, ApJ, 460, 976
Melrose, D. B. 1980, Sol. Phys., 7, 357
Melrose, D. B. 1985, in Solar Radiophysics, eds D. J. McLean & N. R. Labrum, (Cambridge: Cambridge University Press), 177
Melrose, D. B., & Dulk, G. A. 1982, ApJ, 259, 844
Pettersen, B. R. 1980, A&A, 82, 53
Spicer, D. S., Benz, A. O., & Huba, J. D. 1981, Astron. Astroph., 105, 221
Willes, A. J. 1999, Sol. Phys., 186, 319
Willes, A. J., & Robinson, P. A. 1996, ApJ, 467, 465